Title	Anomalous Magnetic Phase Diagram of CeTe under High Pressure
Author(s)	Takaguchi, Hiroaki; Hayashi, Yuya; Matsumura, Takeshi; Umeo, Kazunori; Sera, Masafumi; Ochiai, Akira
Citation	Journal of the Physical Society of Japan , 84 (4) : 044708-1 - 044708-6
Issue Date	2015
DOI	10.7566/JPSJ.84.044708
Self DOI	
URL	https://ir.lib.hiroshima-u.ac.jp/00043718
Right	Copyright (c) 2015 The Physical Society of Japan Copyright (c) 2015 一般社団法人日本物理学会 This is not the published version. Please cite only the published version. この論文は出版社版でありません。引用の際には出版社版をご確認ご利用ください。
Relation	

Anomalous Magnetic Phase Diagram of CeTe under High Pressure

Hiroaki Takaguchi[1], Yuya Hayashi[1], Takeshi Matsumura[1,2] *, Kazunori Umeo[1,3], Masafumi Sera[1,2],
and Akira Ochiai[4]

[1]*Department of Quantum Matter, AdSM, Hiroshima University, Higashi-Hiroshima, Hiroshima 739-8530*
[2]*Institute for Advanced Materials Research, Hiroshima University, Higashi-Hiroshima, Hiroshima 739-8530*
[3]*Cryogenics and Instrumental Analysis Division, N-BARD, Hiroshima University, Higashi-Hiroshima, Hiroshima 739-8526*
[4]*Department of Physics, Graduate School of Science, Tohoku University, Sendai, 980-8578*

We have investigated the anomalous ordered phase of CeTe under high pressure, which has been suggested to be an antiferroquadrupole ordered phase. An anisotropic magnetic phase diagram has been obtained from magnetization and specific heat measurements for the three main field directions along [100], [110], and [111]. We discuss the magnetic phase diagram using a two-sublattice mean-field calculation including antiferromagnetic and antiferroquadrupolar interactions. The anomalous ordered phase can be interpreted as an antiferromagnetic ordered phase, which is strongly affected by the antiferroquadrupolar interaction through the off-diagonal matrix element between the Γ_7 crystal-field ground state and the Γ_8 excited state.

1. Introduction

There is a rich variety of electronic phase transitions in strongly correlated electron systems, where spin, orbital, and charge degrees of freedom play important roles. In rare-earth compounds with relatively localized f-electrons, hybridization with conduction electrons (c-f hybridization) makes the low-temperature phenomenon more interesting through the competition between the Ruderman-Kittel-Kasuya-Yosida (RKKY)-type interaction and the Kondo effect; the former mediates the interionic interaction between localized moments, leading to ordered phases of various types of multipole moment, whereas the latter screens the localized moments and leads to anomalous heavy fermion states. Recently, nontrivial phenomena originating from the interplay between nondipolar degrees of freedom and the Kondo effect have been of special interest.[1–3]

Ce monochalcogenides, CeX_c (X_c=S, Se, Te), with the NaCl-type structure, have been considered as simple antiferromagnets with only the magnetic dipolar degree of freedom of the Γ_7-doublet crystalline electric field (CEF) ground state. One reason is that the Γ_8-quartet excited state well isolated at 32 K for CeTe, 116 K for CeSe, and 140 K for CeS.[4–8] Another is that the ordered moments of the antiferromagnetic (AFM) ordering of these compounds, with T_N = 1.9, 5.4, and 8.4 K for CeTe, CeSe, and CeS, respectively, can basically be understood as originating from the Γ_7 ground state. The magnitudes of the ordered moments, 0.3, 0.56, and 0.57 μ_B for CeTe, CeSe, and CeS, respectively, are roughly consistent with 0.71 μ_B for the Γ_7 CEF eigenstate. The reductions of the moments may be due to the Kondo effect, except for the much reduced value for CeTe, which has not been resolved yet.[9,10]

In CeTe, however, it has recently been found that the quadrupolar moment of the Γ_8 excited state plays an important role in the ordering phenomenon, especially under high pressure.[11] The magnetic phase diagram at 1.2 GPa is quite reminiscent of CeB_6,[12] a typical system of antiferroquadrupolar (AFQ) ordering; the transition temperature increases significantly with increasing magnetic field. This pressure-induced phenomenon in CeTe can be associated with the level lowering of the Γ_8-quartet under high pressure, which contributes to the increase in multipolar degrees of freedom. In CeTe, therefore, in combination with the enhanced Kondo effect at high pressures due to increased hybridization,[13] a novel type of quantum critical behavior using the multipolar degrees of freedom could be expected.

To show if the quadrupole order is realized in CeTe under high pressure, investigation of anisotropy is of essential importance, which was not performed in a previous study.[11] Also, it is important to measure specific heat since it is more sensitive for detecting thermodynamic anomalies and there might be a phase transition, which is missed in magnetization. In the present paper, we report on the magnetization of CeTe at 1.2 GPa for $\boldsymbol{H} \parallel$ [110] and [111], which completes the previous report for $\boldsymbol{H} \parallel$ [100]. Specific heat results under high pressure in magnetic fields for the three main field directions are also presented. We construct a magnetic phase diagram from these measurements and discuss the ordered phases using a two-sublattice mean-field calculation taking into account magnetic dipolar and electric quadrupolar interactions.

2. Experimental Procedure

Magnetization measurement was performed by a standard extraction method using a 15 T cryomagnet system. We used a CuBe piston-cylinder-type high-pressure clamp-cell.[14] Daphne oil was used as a pressure-transmitting medium. Pressure at low temperature was determined by measuring the superconducting transition

*tmatsu@hiroshima-u.ac.jp

temperature of Sn.

Specific heat under high pressure was measured using an AC calorimeter with a Bridgman anvil cell.[15,16] The shaped sample was wrapped by indium and was placed in a CuBe gasket. Indium works as a pressure-transmitting medium and also as a pressure monitor. Pressure was determined from the superconducting transition temperature of indium, which could be identified as an anomaly in the total heat capacity.

3. Experimental Results

3.1 Magnetization

Figure 1 shows the temperature dependences of magnetization at 1.2 GPa for $H \parallel [110]$ and $H \parallel [111]$. The results for $H \parallel [100]$ have already been reported in Ref. 11. At low fields below 1 T, as for $H \parallel [100]$, an upturn at 3 K and a cusp at 2 K are clearly separated, indicating two successive transitions. The cusp anomaly at 2 K shifts to lower temperatures with increasing field. This shows that the anomaly reflects an AFM order. By contrast, the transition temperature for the upturn anomaly at 3 K increases with increasing field, which is also the case for $H \parallel [100]$. All these features are commonly observed for the three main field directions.

At 1.2 GPa, the magnetization increases and the magnetic anisotropy is weakened as compared with those at ambient pressure. At 5 K and 14.5 T, for example, the magnetization values at ambient pressure are $M_{[100]} = 1.14$ μ_B, $M_{[110]} = 1.27$ μ_B, and $M_{[111]} = 1.32$ μ_B. At 1.2 GPa, these values change to $M_{[100]} = 1.36$ μ_B, $M_{[110]} = 1.43$ μ_B, and $M_{[111]} = 1.40$ μ_B. These changes in values and anisotropy can be understood within the Γ_7–Γ_8 CEF model; when the energy of the Γ_8 level decreases at high pressures, the contribution from the Γ_8 increases. This leads to the increase in magnetization and the decrease in magnetic anisotropy.

3.2 Specific heat

Figures 2, 3, and 4 show the temperature dependences of specific heat under high pressures for $H \parallel [100]$, $H \parallel [110]$, and $H \parallel [111]$, respectively. All these data can be treated as magnetic specific heat. The specific heat of LaTe, a nonmagnetic reference compound, is only ~ 0.6 J·mol^{-1}K^{-1} at 8 K, which can be neglected in the present temperature range.

At 0.7 GPa, at zero field, a clear λ-shaped anomaly corresponding to the AFM order is observed at $T_N = 2.3$ K, which is larger than $T_N = 1.9$ K at ambient pressure. One of the new findings in the present study in specific heat is the existence of another phase transition below T_N in magnetic fields. As shown in the data for 0.7 GPa for $H \parallel [100]$, the single anomaly at the AFM transition splits above 2 T. Below the large λ-shaped anomaly in $C(T)$, which reflects the main AFM ordering, a weak peak is clearly observed and shifts to lower temperatures with increasing field. This transition is not detected in magnetization probably because the anomaly is too small. This weak peak in $C(T)$ below the sharp peak at T_N exists also at ambient pressure in the same way as that at 0.7 GPa, although the data is not shown here.
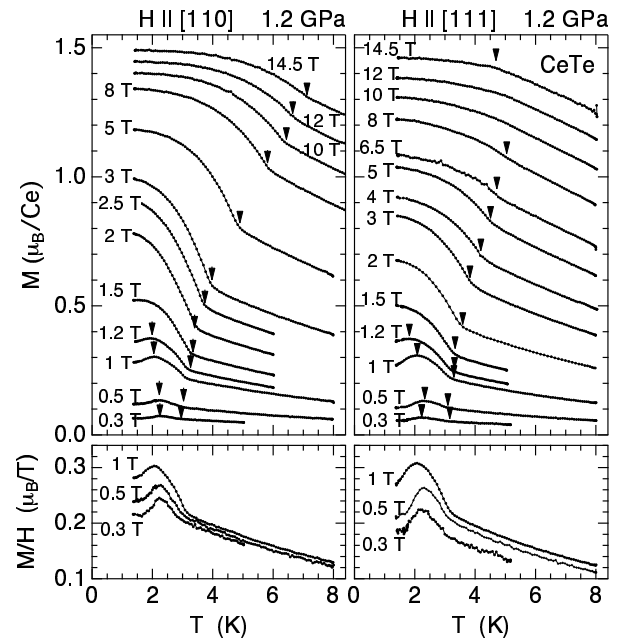
Fig. 1. Temperature dependences of magnetization for $H \parallel [110]$ and $[111]$ at 1.2 GPa. Arrows indicate the transition temperatures. The low field region is shown in the bottom panels in the form of M/H.

At 1.2 GPa and zero field, the two transitions are clearly detected as λ-shaped anomalies in $C(T)$. One is at $T_{N1} = 2.8$ K and the other is at $T_{N2} = 1.9$ K, corresponding to the upturn and cusp anomalies in the $M(T)$ curve, respectively. Although there are slight differences in transition temperatures between the $M(T)$ and $C(T)$ data because of the different pressure settings, the field dependences of the transition temperatures are consistent with each other. At 1.2 GPa, as well as at 0.7 GPa, for $H \parallel [100]$ and $[110]$, another phase transition seems to exist below T_{N1} in magnetic fields, which can be recognised as a weak peak below the λ-shaped anomaly at T_{N1}. However, the weak peak soon broadens out at weaker fields than at 0.7 GPa.

A marked change occurs at 1.8 GPa. The separate transitions at 1.2 GPa change to almost a single transition with a very sharp peak at 3 K, leaving a tiny hump anomaly slightly above the sharp peak. For $H \parallel [100]$, with increasing field, the sharp peak seems to shift to lower temperatures with significantly decreasing the peak height. The weak hump anomaly at zero field, by contrast, seems to shift to higher temperatures with increasing the peak height and the sharpness. At 0.75 T, another anomaly seems to exist between the two anomalies indicated by the arrows. Also, for $H \parallel [110]$, with increasing field, the sharp peak at zero field seems to gradually disappear, whereas the weak hump anomaly grows to the main λ-shaped anomaly. The behavior of specific heat at 2.5 GPa, although the data are not shown here, is almost the same as that at 1.8 GPa.

For $H \parallel [111]$ at 1.8 GPa, we can clearly observe double peaks in $C(T)$ at high fields, which is in contrast to the cases for $H \parallel [100]$ and $[110]$. The sharp peak at zero field seems to be connected to the weaker peak at
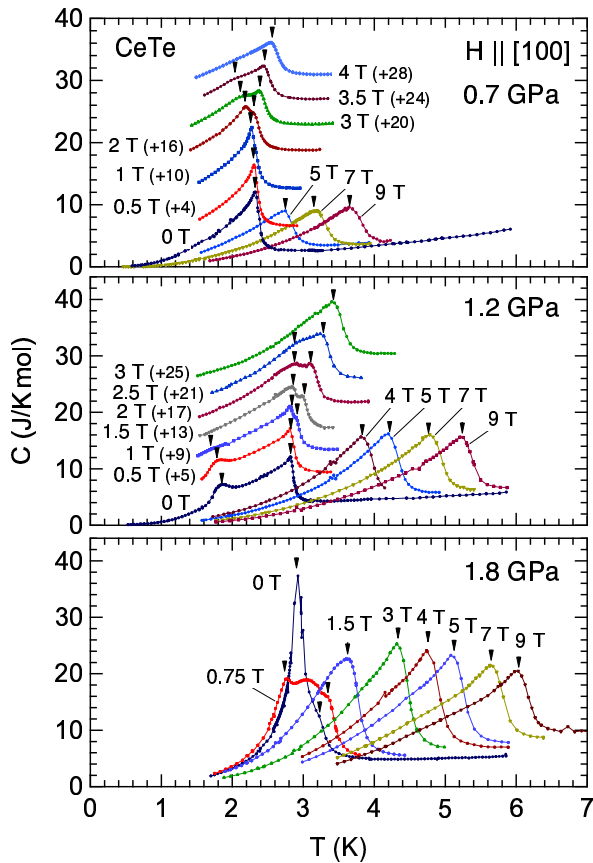
Fig. 2. (Color online) Temperature dependences of specific heat under high pressures for $H \parallel [100]$. The data are vertically shifted as indicated in the parentheses.
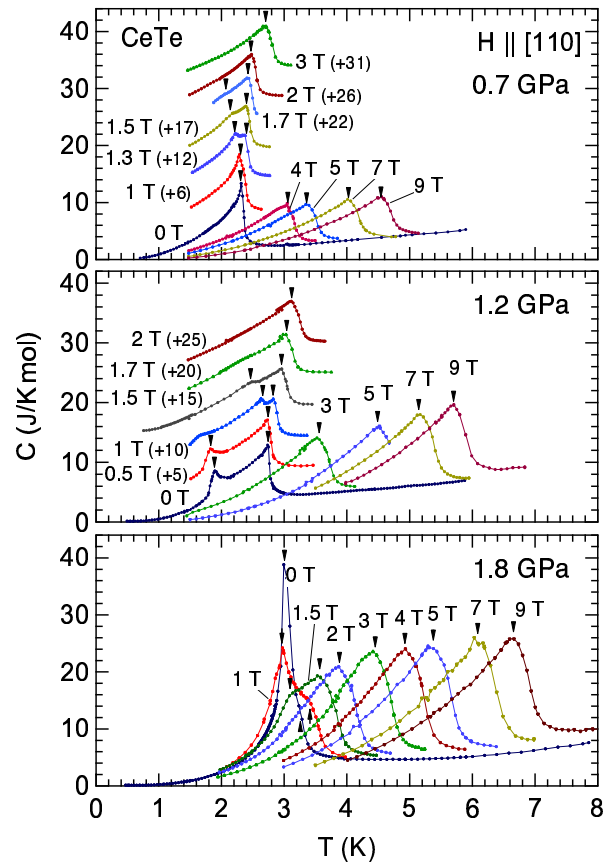
Fig. 3. (Color online) Temperature dependences of specific heat under high pressures for $H \parallel [110]$. The data are vertically shifted as indicated in the parentheses.

lower temperature in high fields, whereas the weak hump anomaly at zero field seems to be connected to the main λ-shaped peak at higher temperature in high fields.

Finally, in Fig. 5, we show the temperature dependences of magnetic entropy at zero field, which was deduced from the $C(T)$ data for the $H \parallel [100]$ pressure setting. At ambient pressure (0 GPa), the released entropy at T_N=1.9 K is less than $R \ln 2$, which is probably associated with the moment reduction of the Γ_7 ground state. With increasing pressure, however, the released entropy at T_N increases and exceeds $R \ln 2$ above 1.2 GPa. It is also noted that the entropy around 4 K, which is just above T_N and well below the CEF splitting of 32 K at 0 GPa, increases with increasing pressure and exceeds $R \ln 2$. This increase cannot be explained by assuming the Γ_8 excited state as being kept at 32 K. It is associated with the level lowering of the Γ_8 state. However, in spite of the level lowering, the increase in entropy stops at 2.5 GPa. This could be due to the enhancement in the Kondo effect.

3.3 Magnetic phase diagram

Figure 6 shows the magnetic phase diagram of CeTe under high pressure determined from the anomalies in magnetization and specific heat. In actual measurements, since the pressure settings are different between the magnetization and the specific heat, we cannot avoid

slight shifts in the observed transition temperatures even though the nominal pressure is the same. These shifts have been corrected in Fig. 6 so that the transition temperatures are consistent between magnetization and specific heat measurements.

The phase diagrams at ambient pressure for the three field directions are consistent with those of the previous report.[10] The AFM ordered phase at zero field and ambient pressure is named phase I. The transition temperature of phase I decreases with increasing magnetic field. Phase I soon changes to phase II at around 1 T for $H \parallel [100]$ and [110], whereas it survives up to 4 T for $H \parallel [111]$. The high-field phases are named phase IV, where the upturn anomaly is clearly observed in magnetization, which means that the transition temperature increases with increasing field. It is noted that, for $H \parallel [100]$, the high-field phase above 8 T is named phase III in Ref. 10. Phase IV is possibly located at high fields above 15 T at 100 mK for $H \parallel [100]$. Since the boundary, or the difference, between phases III and IV is unclear at this stage, phase IV is written in the parenthesis in Fig. 6. As discussed later, we consider that phase IV should be continuously connected up to high pressures for any field direction.

The Néel temperature at zero field initially increases with increasing pressure: from 1.9 K at ambient pressure to 2.4 K at 1 GPa. Only one transition is observed below
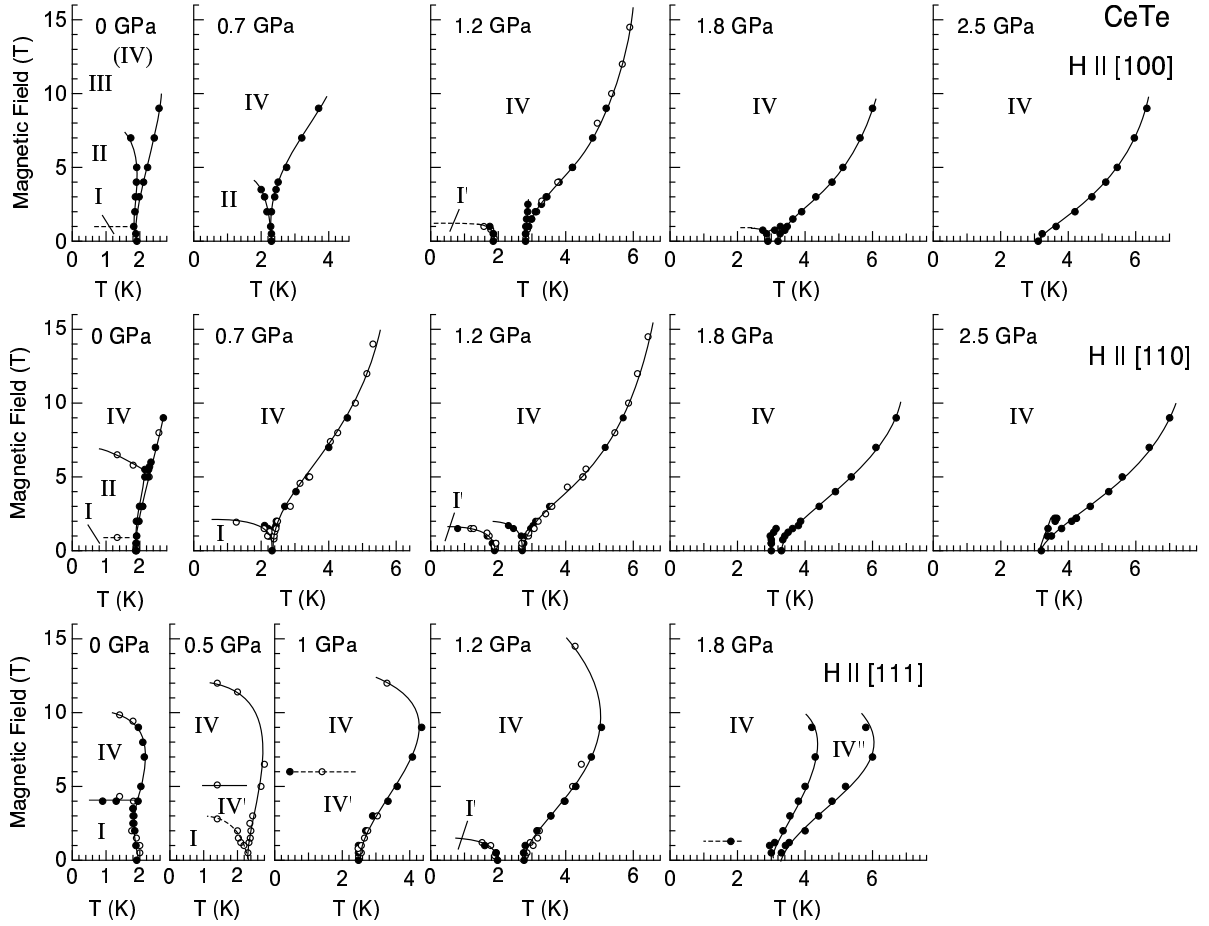
Fig. 6.   Magnetic phase diagram of CeTe under high pressures for three field directions along [100], [110], and [111]. Open and solid circles are from magnetization and specific heat measurements, respectively. The lines are guides for the eye.

1 GPa. With increasing magnetic field, phase IV soon appears and the transition temperature of phase IV is significantly enhanced by the applied field, which is reminiscent of an AFQ order. At 0.5 GPa for $\boldsymbol{H} \parallel [111]$, there seems to be another phase between phases I and IV, which is named phase IV' in that the transition temperature increases with increasing field. At 0.7 GPa, the boundary between phases I and II for $\boldsymbol{H} \parallel [100]$ and that between phases II and IV for $\boldsymbol{H} \parallel [110]$ were difficult to detect. Also, for $\boldsymbol{H} \parallel [111]$ at 1 GPa, the boundary between phases I and IV' could not be detected.

At 1.2 GPa, the AFM transition at zero field splits into two transitions at $T_{N1}=2.8$ K and $T_{N2}=2$ K. The higher transition temperature T_{N1} is more significantly enhanced in magnetic fields than at lower pressures. The phase boundary between phase IV and the paramagnetic phase is isotropic at low fields below 2 T. Above 5 T, however, the anisotropy of T_{N1} is clearly observed; T_{N1} is highest for $\boldsymbol{H} \parallel [110]$ and lowest for $\boldsymbol{H} \parallel [111]$. By contrast, T_{N2} decreases with increasing field. The phase diagram at 1.2 GPa reminds us of the typical phase diagram of AFQ and AFM orderings in CeB$_6$. This is the reason why we proposed an AFQ order in the previous report.[11]

At 1.8 GPa, the low-temperature transition at T_{N2} seems to disappear and only the transition at T_{N1} re-

mains, which seems to be split slightly. Note that only phase IV for $\boldsymbol{H} \parallel [111]$ is clearly separated into two regions in magnetic fields, which are named phases IV and IV''. Finally, at 2.5 GPa, the split transition at zero field at 1.8 GPa seems to merge into a single transition at $T_N=3.2$ K.

4. Discussion

4.1 Mean-field calculation

Although we have interpreted phase IV as an AFQ ordered phase, it is unclear what aspect of the ordered state corresponds to the AFQ state. To shed light on this question, we discuss the experimental phase diagram by considering the following Hamiltonian in the two-sublattice mean-field model:

$$\mathcal{H} = \sum_{i} \left\{ \mathcal{H}_{\mathrm{CEF}} - g\mu_{\mathrm{B}} \boldsymbol{J}(i) \cdot \boldsymbol{H} \right\} - \sum_{i,j} K_{\mathrm{D}} \boldsymbol{J}(i) \cdot \boldsymbol{J}(j)$$
$$- \sum_{i,j} \sum_{\gamma} K_{\mathrm{Q}} O_{\gamma}(i) O_{\gamma}(j) \quad (\gamma = yz, zx, xy), \qquad (1)$$

where $\mathcal{H}_{\mathrm{CEF}}$ is the cubic CEF providing the Γ_7 ground state. Magnetic dipole and electric quadrupole exchange interactions are represented by K_{D} and K_{Q}, respectively. We take into account quadrupolar interaction only between O_{xy}-type quadrupolar moments, where O_{xy} is defined as $\sqrt{3}(J_x J_y + J_y J_x)/2$, and so on. We assumed
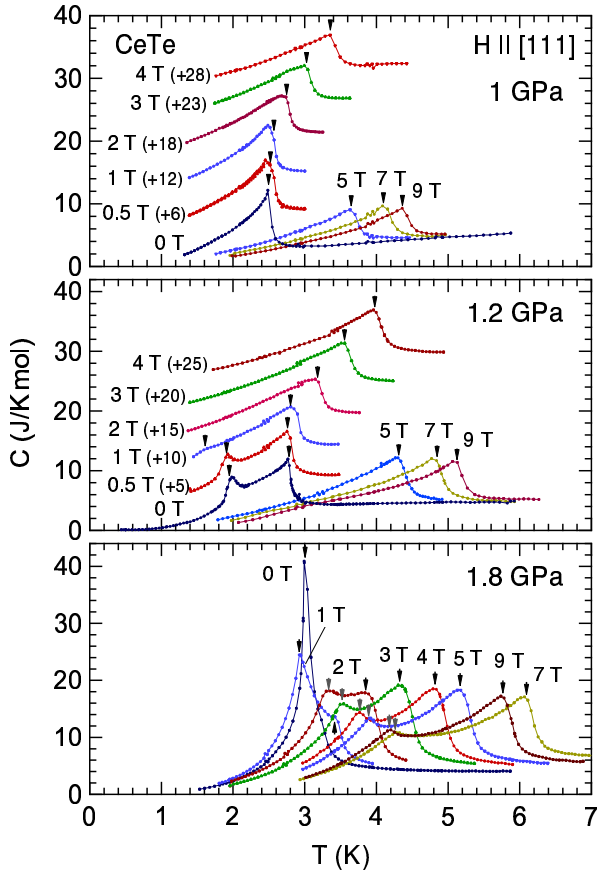
Fig. 4. (Color online) Temperature dependences of specific heat under high pressures for $H \parallel [111]$. The data are vertically shifted as indicated in the parentheses.
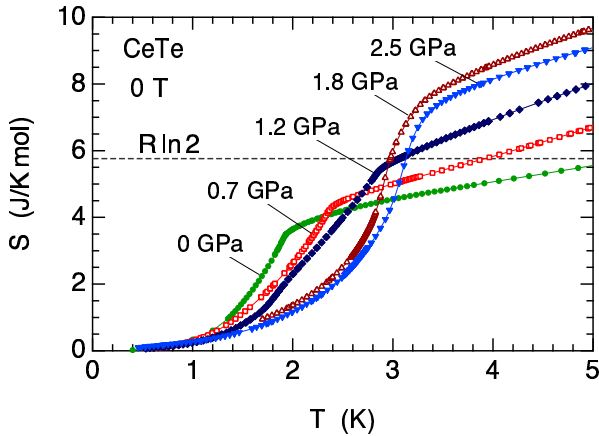
Fig. 5. (Color online) Temperature dependences of magnetic entropy under high pressure at zero field deduced from the specific heat data for the $H \parallel [100]$ pressure setting.

Fig. 7. Calculated magnetic phase diagram for the two-sublattice mean-field model described in the text.

tained by comparing the free energies of the eigenstates.

At $\Delta = 30$ K, corresponding to ambient pressure, an AFM order occurs with $T_{\mathrm{N}} = 2$ K. In the calculation, this phase is named as phase A, where the dipole moment is oriented along the [111] axis, as is naturally expected from the Γ_7 ground state. It is noted that, in Fig. 7, the direction of the AFM moment in phase A is $[1\bar{1}1]$ for $H \parallel [110]$ and $H \parallel [111]$ since it is more perpendicular to the field direction than other $\langle 111 \rangle$-equivalent directions, and therefore it is more stable in magnetic fields. For $H \parallel [100]$, four magnetic domains are equivalent with respect to the field direction.

When the field is applied along [100], the AFM moment $\boldsymbol{m}_{\mathrm{AF}}$ soon changes its direction to [011], which is phase C. This is because the AFM moments prefer to be perpendicular to the magnetic field. At high fields for $H \parallel [100]$, the AFM moment changes its direction to [001], which is phase B. For $H \parallel [110]$, phase A changes directly to phase B ($\boldsymbol{m}_{\mathrm{AF}} \parallel [001]$) without passing through phase C ($\boldsymbol{m}_{\mathrm{AF}} \parallel [1\bar{1}0]$). In phase B, the moments are antiferromagnetically oriented along [001] with the ferromagnetic component along the field direction. It is noted that, in phase B, the energy gain of the ordered state is provided by the O_{xy}-type AFQ moment

(O_{zx} for $\boldsymbol{H} \parallel [100]$ and $O_{yz} + O_{zx}$ for $\boldsymbol{H} \parallel [110]$), which is induced in magnetic fields through the mixing with the Γ_8 excited state.[17] Thus, phase B could be called an AFQ phase. With decreasing Δ, corresponding to the increase in pressure, T_N at zero field increases and the transition temperature from phase B to the paramagnetic phase increases. These results are due to the level lowering of the Γ_8 excited state.

In the calculated phase diagram, the single AFM transition changes to the double transition at $\Delta = 12$ K, where phase B is realized at zero field. In this phase B at zero field, only the magnetic dipole moment along [001] is ordered and the O_{zx} AFQ is zero. Since there is no energy gain from the AFQ order, the appearance of phase B at zero field is due to the Γ_8 contribution to the magnetic dipole moment. This is consistent with the fact that the magnetic easy axis of the Γ_8 state is the fourfold axis. In magnetic fields in phase B, O_{xy}-type AFQ moments are induced through the off-diagonal element between Γ_7 and Γ_8 CEF states, leading to the energy gain in the AFQ interaction and the increase in the transition temperature.[17]

For $\boldsymbol{H} \parallel [111]$, phase A corresponds to the AFM ordered phase with $\boldsymbol{m}_{AF} \parallel [1\bar{1}1]$. In phase A, although the O_{xy}-type AFQ moments are induced while the AFM moments are canted to the field direction, the transition temperature does not increase when $\Delta = 30$ and 24 K. Starting from $\boldsymbol{m}_{AF} \parallel [1\bar{1}1]$ at zero field, only a tiny amount of O_{xy}-type AFQ moments are induced for $\boldsymbol{H} \parallel [111]$, leading to a negligibly small increase in T_N. This is because the energy gain by the O_{xy}-type AFQ moments is insufficient to overcome the Zeeman energy, which is in contrast to the cases for $\boldsymbol{H} \parallel [100]$ and [110]. At $\Delta = 18$ K, however, a new phase, named phase D, appears at higher temperatures, where the AFM moment is oriented parallel to [111], the field direction. In this phase, the order parameter is the $O_{yz} + O_{zx} + O_{xy}$ AFQ moment, which means that long and short magnetic dipole moments are oriented alternately along the [111] axis. In this sense, phase D could also be called an AFQ phase.

Note that, at zero field, there is no difference in energy between phases A and D; there is no AFQ moment at zero field. In magnetic fields, however, the AFQ moment is induced and there is a difference in energy as separated by the phase boundary between phases A and D.

At $\Delta = 12$ K for $\boldsymbol{H} \parallel [111]$, phase B appears in the low-field region. Phase D, however, gains more energy of the AFQ interaction in magnetic fields than phase B. Phase A' at high fields for $\boldsymbol{H} \parallel [111]$ is similar to phase A with a slight difference in the canted magnetic structure.

4.2 Comparison with the experiment

We see that the mean-field calculation qualitatively explains the behavior of the phase boundary between phase IV and the paramagnetic phase, especially for $\boldsymbol{H} \parallel [100]$ and [110]. Firstly, the increase in T_{N1} in magnetic fields, which is more enhanced at high pressures, is reproduced in the calculation. Secondly, the successive phase transitions at zero field, as observed experimentally at 1.2 GPa, also occur in the calculation for $\Delta = 12$ K. These results

show that the ordered phases of CeTe at high pressures are strongly associated with the level lowering of the Γ_8 excited state.

Phase A in the calculation, with $\boldsymbol{m}_{AF} \parallel [111]$, which soon becomes unstable in magnetic fields, is reasonably suggested to correspond to phase I in the experiment. It is also suggested that phase B in the calculation corresponds to phase IV in the experiment. The energy gain of phase B at high magnetic fields, with $\boldsymbol{m}_{AF} \parallel [001]$ for $\boldsymbol{H} \parallel [100]$ and [110], comes from the AFQ interaction through the off-diagonal matrix element of O_{yz} and O_{zx} between Γ_7 and Γ_8. This phase is, therefore, more stabilized with the level lowering of the Γ_8 state. At zero field, however, since the O_{zx} AFQ moment is not induced, phase B has no energy gain from the AFQ interaction. Then, phase A has lower energy than phase B at zero field. However, when the Γ_8 level drops down, phase B can be realized at zero field as an intermediate phase at higher temperatures. This is the case for $\Delta = 12$ K in the calculation, and is expected to be the case for 1.2 GPa in the experiment.

By contrast, the calculated results for $\boldsymbol{H} \parallel [111]$ are not very much consistent with the experiment. Phase I soon disappears in magnetic fields in the experiment, whereas phase A survives up to high fields in the calculation. In the experiment, phase IV at high fields seems to be continuously connected for all the field directions from $\boldsymbol{H} \parallel [100]$ to $\boldsymbol{H} \parallel [110]$ as in the AFQ phase of CeB$_6$.[18] However, in the present mean-field calculation for CeTe, phase B does not appear at high fields for $\boldsymbol{H} \parallel [111]$. One possible reason for this discrepancy might be that the two-sublattice model is not sufficient to describe the ordered phases with $\boldsymbol{q} = (1/2, 1/2, 1/2)$ in the NaCl-type compound. The two-sublattice model is based on the assumption that the face-centered-cubic lattice of Ce is decoupled to four independent simple-cubic lattice.[19,20] This assumption is valid if the intersite interaction between Ce f-electrons is mediated mainly through the p-orbital of Te. Although the p-f mixing is actually expected to be strong in CeTe, the interaction through the conduction d-electrons, which couples the four sublattices, may not be neglected.[9] Another possible reason for the discrepancy could be that the quadrupolar interaction between O_{20} and O_{22} moments is neglected. Further study by including this interaction will be performed in the future. Detailed structures of the phase diagram such as phases II, III, and IV' are also beyond the scope of the present mean-field calculation.

The AFQ order for $\boldsymbol{H} \parallel [111]$ in calculation appears as phase D, where the AFM moments orient parallel to the field direction [111]. This phase appears at temperatures higher than those of phase A when Δ is decreased, as a result of increased thermal population of the Γ_8 state. The appearance of phase IV'' in the experiment at 1.8 GPa, therefore, could be associated with this phase D in the calculation.

Finally, with respect to the level lowering of the Γ_8 excited state under high pressure, we speculate that it is strongly associated with the *anisotropic c-f hybridization*, which is dependent on the CEF states. We suggest that the Γ_8 state is more strongly hybridized with

the conduction electrons. This effect in CeX$_c$ will be discussed in another paper.

5. Conclusions

We have investigated the anomalous ordered phase of CeTe under high pressure by magnetization and specific heat measurements. The pressure dependence of the magnetic phase diagram for three principal axes has been obtained experimentally. We discussed the phase diagram by comparing with a two-sublattice mean-field calculation and showed that the pressure dependence of the ordered state is strongly associated with the level lowering of the Γ_8 excited state under high pressure. The ordered state at zero field can basically be interpreted as an AFM ordered phase. However, it is strongly affected by the AFQ interaction in magnetic fields through the off-diagonal mixing term between Γ_7 and Γ_8 CEF states. The high-field phase in CeTe at high pressures, therefore, could be called an AFQ ordered phase.

Acknowledgements

1) A. Sakai and S. Nakatsuji, J. Phys. Soc. Jpn. **80**, 063701 (2011).
2) A. Sakai, K. Kuga, and S. Nakatsuji, J. Phys. Soc. Jpn. **81**, 083702 (2012).
3) K. Matsubayashi, T. Tanaka, A. Sakai, S. Nakatsuji, Y. Kubo, and Y. Uwatoko, Phys. Rev. Lett. **109**, 187004 (2012).
4) F. Hulliger, B. Natterer, and H. R. Ott, J. Magn. Magn. Mater. **8**, 87 (1978).
5) H. R. Ott, J. K. Kjems, and F. Hulliger, Phys. Rev. Lett. **42**, 1378 (1979).
6) A. Dönni, A. Furrer, P. Fisher, S. M. Hayden, F. Hulliger, and T. Suzuki, J. Phys: Condens. Matter **5**, 1119 (1993).
7) A. Dönni, A. Furrer, P. Fisher, and F. Hulliger, Physica B **186-188**, 541 (1993).
8) J. Rossat-Mignod, J. M. Effantin, P. Burlet, T. Chattopadhyay, L. P. Regnault, H. Bartholin, C. Vettier, O. Vogt, D. Ravot, and J. C. Achart, J. Magn. Magn. Mater. **52**, 111 (1985).
9) M. Nakayama, H. Aoki, A. Ochiai, T. Ito, H. Kumigashira, T. Takahashi, and H. Harima, Phys. Rev. B **69**, 155116 (2004).
10) M. Nakayama, N. Kimura, H. Aoki, A. Ochiai, C. Terakura, T. Terashima, and S. Uji, Phys. Rev. B **70**, 054421 (2004).
11) Y. Kawarasaki, T. Matsumura, M. Sera, and A. Ochiai, J. Phys. Soc. Jpn. **80**, 023713 (2011).
12) J. M. Effantin, J. Rossat-Mignod, P. Burlet, H. Bartholin, S. Kunii, and T. Kasuya, J. Magn. Magn. Mater. **47&48**, 145 (1985).
13) Y. Hayashi, H. Takaguchi, T. Matsumura, M. Sera, and A. Ochiai, JPS Conf. Proc. **3**, 011035 (2014).
14) Y. Uwatoko, T. Hotta, E. Matsuoka, H. Mori, T. Ohki, J. L. Sarrao, J. D. Thompson, N. Môri, and G. Oomi, Rev. High Pressure Sci. Technol. **7**, 1508 (1998).
15) H. Kubo, K. Umeo, and T. Takabatake, J. Phys. Soc. Jpn. **76**, Suppl. A, 221 (2008).
16) H. Kubo, K. Umeo, K. Katoh, A. Ochiai, and T. Takabatake, J. Phys. Soc. Jpn. **77**, 023704 (2008).
17) K. Hanzawa and T. Kasuya, J. Phys. Soc. Jpn. **53** 1809 (1984).
18) T. Matsumura, T. Yonemura, K. Kunimori, M. Sera, F. Iga, T. Nagao, and J. I. Igarashi, Phys. Rev. B **85**, 174417 (2012).
19) R. Shiina, H. Shiba, and O. Sakai, J. Phys. Soc. Jpn. **68**, 2105 (1999).
20) R. Shiina, H. Shiba, and O. Sakai, J. Phys. Soc. Jpn. **68**, 2390 (1999).